

Calculations on the Kinetics, Thermodynamics, and Selectivity of Methyl Radical Addition to Olefins Coordinated to d^8 and d^0 Transition-Metal Fragments: Two Distinct and Opposite anti-Evans–Polanyi Effects with Potential Practical Implications

Faraj Hasanayn* and Samer Gozem

Department of Chemistry, American University of Beirut, Beirut, Lebanon

Received August 7, 2008

Summary: DFT calculations predict that methyl radical addition to the propene and isobutene adducts of the $[Rh(PCP)]$ and $[(Cp)_2Zr(O^tBu)]^+$ fragments affords different kinetic and thermodynamic products. The regioselectivity in the Zr adducts is predicted to be reversed compared to that in the uncoordinated or the Rh-coordinated systems.

The addition of free radicals to alkenes is an important reaction in synthetic and polymer chemistry.^{1,2} The reaction is known to encounter an intriguing activation barrier, interpretation of which has been a challenging subject for experimental and theoretical research.^{3,4} In a comprehensive analysis of a large data set, Fischer and Radom show that the barrier height of radical addition reactions depends on an interplay of several subtle factors, including an enthalpic term, excited-state correlation, steric effects, and electrophilic and nucleophilic polar effects.⁵ Noticeably, for subsets of related reactions, such as alkyl addition to certain mono- and 1,1-substituted ethylenes,⁵ the kinetics qualitatively follow the Evans–Polanyi relation,⁶ meaning that the more exothermic reactions tend to exhibit smaller barriers.

The ability to manipulate the characteristic reactivity patterns of radical reactions can be important from both fundamental and practical perspectives. For example, Clark calculated that propene coordination to Li^+ lowers the activation energy of methyl addition,⁷ and this could eventually explain the observed puzzling activity of Michl's alkene polymerization systems.⁸ We have been interested in using electronic structure methods to explore the scope by which coordination of unsaturated organic substrates to transition-metal fragments may modify their radical addition reactions, and we recently reported studies

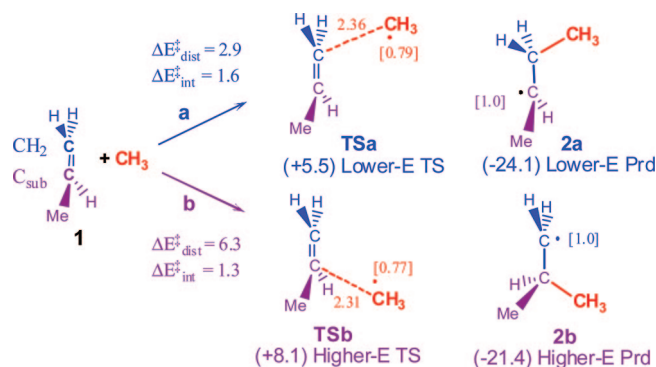


Figure 1. Reaction or activation enthalpies at 298 K and 1 atm of methyl addition to **1**, and associated $\Delta E_{\text{dist}}^{\ddagger}$ and $\Delta E_{\text{int}}^{\ddagger}$ values (relative to the separate reactants; in kcal/mol). Selected parameters are given in Å. Values in brackets are the Mulliken spin densities on the selected atoms or groups.

on alkyl addition to metal-coordinated CO.⁹ Herein we use mostly B3LYP DFT calculations^{10,11} to study how the transition states (TSs) and products of methyl addition to propene (**1**) will change when propene is coordinated to the $[d^8-(\kappa^3\text{-PCP})Rh]$ (**Rh**; PCP = 1,3- $C_6H_3(CH_2PMe_2)_2$) and $[d^0-(\eta^5\text{-Cp})_2Zr(O^tBu)]^+$ (**Zr**) fragments. On consideration of addition to (a) the terminal (CH_2) and (b) the substituted (C_{sub}) carbons of the double bond in **1** (Figures 1–3), the results demonstrate that coordination introduces markedly different effects on the activation and reaction energies of alkyl addition to **1** that have potentially very significant implications in the theory and practice of free radical additions to olefins.

The results for the reaction of free propene are summarized in Figure 1. In line with prior studies,^{4a,12} we calculate CH_2 in **1** to have a greater thermodynamic methyl affinity (-24.4) than does C_{sub} (-21.4 ; ΔH° values in kcal/mol). For this molecule, addition to CH_2 encounters a smaller activation enthalpy than does C_{sub} (5.4 vs 8.1 kcal/mol). Shaik^{4a} and Radom¹² related the kinetic preference for CH_2 to a greater enthalpic term that coincides with a more favorable (larger) spin density distribution on CH_2 in the triplet state of **1**. For the sake of discussion in the present study, we find it useful to analyze the variations in the barrier heights using the activation strain model built on a

*To whom correspondence should be addressed. E-mail: fh19@aub.edu.lb.

(1) Giese, B. *Radicals in Organic Syntheses: Formation of Carbon-Carbon Bonds*; Pergamon: Oxford, U.K., 1986.

(2) Fossey, J.; Lefort, D.; Sorba, J. *Free Radicals in Organic Chemistry*; Wiley: New York, 1995.

(3) (a) Giese, B. *Angew. Chem., Int. Ed.* **1983**, *22*, 573. (b) Zytowski, T.; Fischer, H. *J. Am. Chem. Soc.* **1998**, *119*, 12869. (c) Lalevee, J.; Allonas, X.; Genet, S.; Fouassier, J.-P. *J. Am. Chem. Soc.* **2003**, *125*, 9377.

(4) (a) Shaik, S. S.; Canadell, E. *J. Am. Chem. Soc.* **1990**, *112*, 1446. (b) Shaik, S. S.; Shurki, A. *Angew. Chem., Int. Ed.* **1999**, *38*, 587. (c) Gomez-Balderas, R.; Coote, M. L.; Henry, D. J.; Radom, L. *J. Phys. Chem. A* **2004**, *108*, 2874.

(5) Fischer, H.; Radom, L. *Angew. Chem., Int. Ed.* **2001**, *40*, 1340.

(6) Evans, M. G.; Polanyi, M. *Trans. Faraday Soc.* **1938**, *34*, 11.

(7) (a) Clark, T. *J. Chem. Soc., Chem. Commun.* **1986**, 1774. (b) Clark, T. *J. Am. Chem. Soc.* **2006**, *128*, 11278.

(8) (a) Vyakaranam, K.; Barbour, J. B.; Michl, J. *J. Am. Chem. Soc.* **2006**, *128*, 5610. (b) Vyakaranam, K.; Korbe, S.; Michl, J. *J. Am. Chem. Soc.* **2006**, *128*, 5680.

(9) (a) Hasanayn, F.; Nsouli, N. H.; Al-Ayoubi, A.; Goldman, A. S. *J. Am. Chem. Soc.* **2008**, *130*, 511. (b) Nsouli, N. H.; Mouawad, I.; Hasanayn, F. *Organometallics*. **2008**, *27*, 2004.

(10) Becke, A. D. *Phys. Rev. B* **1988**, *37*, 785.

(11) All calculations were carried out using Gaussian 2003.

(12) Henry, D. J.; Coote, M. L.; Gomez-Balderas, R.; Radom, L. *J. Am. Chem. Soc.* **2004**, *126*, 1732.

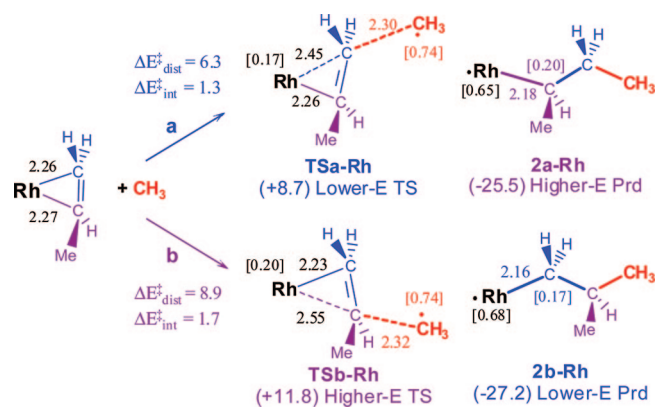


Figure 2. Reaction or activation enthalpies at 298 K of methyl addition to $\mathbf{1-Rh}$, and associated $\Delta E_{\text{dist}}^{\ddagger}$ and $\Delta E_{\text{int}}^{\ddagger}$ values (relative to the separate reactants; in kcal/mol). Selected parameters are given in Å. Values in brackets are the Mulliken spin densities on the selected atoms or groups.

thermodynamic cycle that gives the activation energy (ΔE^{\ddagger}) as the sum of a distortion energy ($\Delta E_{\text{dist}}^{\ddagger}$; defined as the energy needed to distort the equilibrium geometry of the reactants to the respective parameters in the TS) and an electronic interaction component ($\Delta E_{\text{int}}^{\ddagger}$, for the energy change that takes place when the distorted reactants are brought to the TS). As found by others,^{13,14} the greater barrier of addition to C_{sub} arises from a requirement for a greater $\Delta E_{\text{dist}}^{\ddagger}$ value to reach **TSb** (data on the arrows in Figure 1). In this uncoordinated system, $\Delta E_{\text{int}}^{\ddagger}$ is small and positive, and the values are comparable for the two sites. This indicates that no net bonding takes place at the early stages of the reaction, and the requirement for distortion can then be thought of as a means to provide a more favorable electronic environment to begin the C–C bond making process.

Coordination of $\mathbf{1}$ to **Rh** is calculated to be exothermic by 18.0 kcal/mol and affords a conventional η^2 -propene complex ($\mathbf{1-Rh}$) (Figure 2). In this complex, as for free propene, methyl attack on CH_2 has a lower barrier than attack on C_{sub} : 8.7 vs 11.8 kcal/mol. However, the higher energy **TSb-Rh** (involving C_{sub}) gives a thermodynamically more favorable product (**2b-Rh**), with $\Delta H_{\text{sub}}^{\circ} = -27.2$ versus $\Delta H_{\text{CH}_2}^{\circ} = -25.5$ kcal/mol. This new thermodynamic preference is not particularly surprising, since C–C bond formation is coupled to formation of an η^1 -alkyl–Rh bond, which is known to be stronger for primary alkyls (as in **2b-Rh**) compared to secondary alkyls (as in **2a-Rh**).¹⁵ In other words, the greater strength of the resulting Rh–C bond thermodynamically favors addition to C_{sub} , overriding the inherent strength of the C–C bond being formed (which favors addition to CH_2).

Each of the barriers in the reaction of $\mathbf{1-Rh}$ is ca. 3.5 kcal/mol larger than in $\mathbf{1}$. The exothermicities on the other hand are greater in $\mathbf{1-Rh}$. Thus, against simplistic expectations based on the Evans–Polanyi relation, coordination to **Rh** introduces opposite effects on the activation and reaction energy of radical addition to either carbon of $\mathbf{1}$. This seems to follow from major differences in how the respective TSs and products compare in the free and coordinated systems. While $\mathbf{1}$ produces a carbon-centered radical, $\mathbf{1-Rh}$ yields a metal-based radical (Figures 1 and 2); hence, it is only normal for the thermodynamics to be

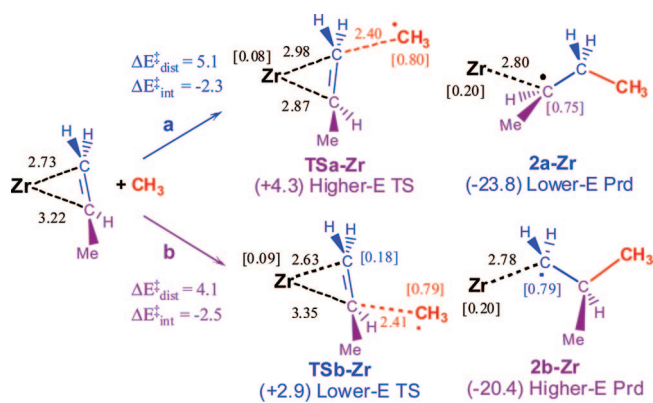


Figure 3. Reaction or activation enthalpies at 298 K of methyl addition to $\mathbf{1-Zr}$, and associated $\Delta E_{\text{dist}}^{\ddagger}$ and $\Delta E_{\text{int}}^{\ddagger}$ values (relative to the separate reactants; in kcal/mol). Selected parameters are given in Å. Values in brackets are the Mulliken spin densities on the selected atoms or groups.

different in the two systems. The greater exothermicity in $\mathbf{1-Rh}$ simply means that the η^2 -alkene to η^1 -alkyl transformation is accommodated favorably in this particular system, and this is much more so in **2b-Rh** (thus switching the thermodynamic preference to addition to C_{sub}).

In contrast to the products, the C–C reaction centers in the free and complexed TSs are more similar than different. Consider the reactions involving CH_2 , for example. In both the free and complexed TSs the C–C bond distance is long (ca. 2.35 Å) and the free radical spin density is still concentrated largely on the attacking methyl group (0.79 in **TSa** vs 0.74 in **TSa-Rh**). This is indicative of minor bond formation or spin transfer in either TS. Comparison of the $\Delta E_{\text{dist}}^{\ddagger}$ and $\Delta E_{\text{int}}^{\ddagger}$ components in the two systems reveals that the increased barrier introduced upon coordination is associated nearly quantitatively with an increase of 3.6 kcal/mol in $\Delta E_{\text{dist}}^{\ddagger}$. On the basis of the TS geometries, the larger $\Delta E_{\text{dist}}^{\ddagger}$ in **TSa-Rh** can be readily attributed to the fact that in order to attain a C–C reaction center similar to that in **TSa**, the incipient carbon (CH_2 in this case) of the coordinated propene has to dissociate from 2.26 Å in $\mathbf{1-Rh}$ to 2.45 Å in **TSa-Rh**. This selectively adds an extra term to $\Delta E_{\text{dist}}^{\ddagger}$ in **TSa-Rh**, which in the absence of a compensating bonding energy in $\Delta E_{\text{int}}^{\ddagger}$ leads to a larger barrier. Because $\mathbf{1}$ binds to **Rh** symmetrically, the proposed role for ligand dissociation as a source for an increased barrier height of reaction should be equally applicable to **TSb-Rh** (involving C_{sub}). This can account for the larger barrier height in the coordinated C_{sub} compared to the free C_{sub} (11.8 vs 8.1 kcal/mol) and, in turn, for the fact that the kinetic preference for CH_2 does not change upon coordination to the given fragment. Elucidation of the advantages of alkene dissociation in reaching the TS requires a thorough analysis of the electronic factors pertinent to C–C bond making, such as the effects on the frontier molecular orbitals involved in the reaction,^{9a} and is beyond the scope of the present communication.

The above effects introduced upon coordination of $\mathbf{1}$ to **Rh** are essentially reversed when $\mathbf{1}$ is coordinated to $[\text{Cp}_2\text{Zr}(\text{O}^i\text{Bu})]^+$ (**Zr**). In accord with prior calculations¹⁶ and NMR observations,^{17,18} $\mathbf{1}$ is calculated to bind to **Zr** in an asymmetric mode that places

(13) Arnaud, R.; Subra, R.; Barone, V.; Lelj, F.; Olivella, S.; Sole, A.; Russo, N. *J. Chem. Soc., Perkin Trans. 2* **1986**, 1517.

(14) Delbecq, F.; Ilavsky, D.; Anh, N. T.; Lefour, J. M. *J. Am. Chem. Soc.* **1985**, *107*, 1623.

(15) (a) Jones, W. D.; Hessel, E. T. *J. Am. Chem. Soc.* **1993**, *115*, 554. (b) Bennett, J. L.; Wolczanski, P. T. *J. Am. Chem. Soc.* **1997**, *119*, 10696.

(16) Zhao, H.; Ariafard, A.; Lin, Z. *Inorg. Chim. Acta* **2006**, *359*, 3527.

(17) (a) Stoebenau, E. J.; Jordan, R. F. *J. Am. Chem. Soc.* **2006**, *128*, 8162. (b) Stoebenau, E. J.; Jordan, R. F. *J. Am. Chem. Soc.* **2006**, *128*, 8638.

(18) Vatamanu, M.; Stojcevic, G.; Baird, M. C. *J. Am. Chem. Soc.* **2008**, *130*, 454.

Zr closer to CH₂ (2.73 Å) than to C_{sub} (3.22 Å, Figure 3). The binding enthalpy between **1** and **Zr** (−13.7 kcal/mol) is reduced compared to that for **Rh** (−18.0 kcal/mol), but the calculated free energy of coordination still comes negative (−2.2 kcal/mol; at 298 K).

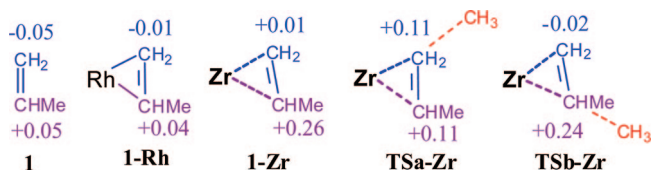
In **1-Zr**, the barrier of methyl addition to CH₂ (4.3 kcal/mol) is smaller than the respective barrier in **1** (5.5 kcal/mol). Remarkably, however, **TSb-Zr** for addition to C_{sub} is predicted to be 1.5 kcal/mol below **TSa-Zr**, thereby leading to a reversed regioselectivity compared to the uncoordinated **1**. Even more striking, a greater kinetic preference for C_{sub} (involving CMe₂ this time) is found for the isobutene adduct of **Zr**, with $\Delta H^{\ddagger}_{\text{CH}_2} = 8.3$ and $\Delta H^{\ddagger}_{\text{sub}} = 6.3$ kcal/mol. The respective barriers in free isobutene are 5.5 and 10.8 kcal/mol. Similar results are calculated for the propene and isobutene adducts of [Cp₂Zr(Me)]⁺, and the conclusions obtained for **1-Zr** are not changed when solvent effects are included as a CH₂Cl₂ continuum, or when the density functional or the basis set is changed. Furthermore, calculations on methyl addition to the isobutene adduct of the model [d⁰-ZrCl₃]⁺ fragment (which also exhibits asymmetric coordination)¹⁹ predict a reversed regioselectivity at the B3LYP-DFT level (used to study **1-Zr**) as well as the coupled cluster correlated ab initio levels of theory (CCSD and CCSD-T; see the Supporting Information).

Analysis of $\Delta E^{\ddagger}_{\text{dist}}$ and $\Delta E^{\ddagger}_{\text{int}}$ can be helpful in accounting for the new reactivity pattern of **1-Zr**. First, and unlike the case for **1** or **1-Rh**, $\Delta E^{\ddagger}_{\text{int}}$ in the reaction of **1-Zr** is negative (ca. −2.4 kcal/mol in both TSs; Figure 3). This is most likely the result of an attractive ion-induced-dipole force along the potential energy surface due to the positive charge of **1-Zr**. Such force is expected to apply to the potential energy surface of both CH₂ and C_{sub} and should therefore play a role in lowering the two respective barriers compared to **1** but not in reversing the regioselectivity. Consistently, the calculated barriers of methyl addition to CH₂ and C_{sub} of the Li⁺ adduct of **1** are reduced compared to the uncomplexed **1**, and they are associated with negative $\Delta E^{\ddagger}_{\text{int}}$ values, but the regioselectivity remains normal.

To address the reversed regioselectivity in **1-Zr**, we inspect $\Delta E^{\ddagger}_{\text{dist}}$. For methyl addition to CH₂, $\Delta E^{\ddagger}_{\text{dist}}$ (5.1 kcal/mol) is larger than the respective $\Delta E^{\ddagger}_{\text{dist}}$ in the uncomplexed propene (2.9 kcal/mol). As in **1-Rh**, this can be related to an extra energy input needed to dissociate the Zr–CH₂ bond from 2.73 to 2.98 Å to be able to attain **TSa-Zr**. Obviously, because **1** binds to **Zr** in an η¹ mode, a smaller degree of dissociation (from 3.22 to 3.35 Å) will be required to make C_{sub} available for the methyl radical in **TSb-Zr**. Surprisingly, however, $\Delta E^{\ddagger}_{\text{dist}}$ in **TSb-Zr** is 2.2 kcal/mol smaller than in the uncomplexed C_{sub}, where the extra metal–ligand dissociation is not even applicable. This implicates a genuine difference in the way the methyl radical interacts with C_{sub} in **1-Zr** compared with the uncomplexed C_{sub}, which allows **TSb-Zr** to be reached without the need for much restructuring in the olefin moiety.

A straightforward interpretation of the new reaction conditions in **TSb-Zr** can be based on polar effects. On the basis of the characteristic ¹³C NMR spectra of complexes related to **1-Zr**,

Scheme 1. Total Mulliken Charge on the CH₂ and CHMe Units of Propene in the Specified Species



Jordan deduced that asymmetric coordination of an olefin such as **1** to a positively charged fragment such as **Zr** builds positive charge on C_{sub} and negative charge on CH₂.¹⁷ More recently, Baird has argued that in such complexes C_{sub} should simply behave as a carbocation.¹⁸ To avoid known artifacts in partitioning charge in CH bonds,²⁰ we analyze in Scheme 1 the calculated total Mulliken charge on the CH₂ and CHMe units of propene in the species relevant to the discussion. For these units, essentially identical charges are obtained by the Mulliken and the Weinhold (NBO) schemes.

In **1** and **1-Rh** the individual units are neutral. In **1-Zr**, on the other hand, the charge on CHMe is +0.26. A buildup of positive charge on the incipient carbon of a double bond can play a role in lowering the barrier to methyl addition by (i) reducing the repulsion between the SOMO of the methyl radical and the filled π-MO, and (not independently) (ii) increasing bonding between the SOMO and the π-MO. Of course, for such frontier orbital modifications to activate C_{sub}, the positive charge has to apply to the TS and not only to the reactant. Indeed, in **TSb-Zr** the asymmetry is retained (Figure 3), and the charge on CHMe remains substantially positive (+0.24). Interestingly, CH₂ in **1-Zr** is calculated to be neutral rather than anionic, which can be consistent with a small degree of covalency in the relatively long Zr–CH₂ bond (2.73 Å). More importantly, in **TSa-Zr** the asymmetry in the Zr–alkene bond is gone, and CH₂ now acquires a positive charge of +0.11. By the above argument, a negative charge on CH₂ in the TS would have probably greatly disfavored addition to CH₂.

In summary to this section, the calculations provide evidence that the characteristic regioselectivity of methyl addition to **1** reverses when **1** coordinates to **Zr**. This seems to follow from the unconventional nature of the bond between **1** and **Zr**, which (i) makes CH₂ spatially less accessible to the methyl radical than C_{sub} (thus selectively disfavoring addition to CH₂) and (ii) selectively builds positive charge on C_{sub} (thus creating a more favorable environment at C_{sub} to begin C–C bond making).

Finally, the products in the reaction of **1-Zr** have long Zr–alkyl bonds (ca. 2.8 Å) in which the spin density is concentrated on the carbon end of the Zr–C bond (Figure 3). While a small covalency in such bonds may not be ruled out, these unconventional products are more like loose **Zr** adducts of the uncoordinated isomeric butyl radicals. Accordingly, **2a-Zr** resulting from methyl addition to CH₂ is calculated to be the thermodynamic product ($\Delta H^{\circ}_{\text{CH}_2} = -24.1$ kcal/mol vs $\Delta H^{\circ}_{\text{sub}} = -19.5$ kcal/mol). This means that in the reaction of **1-Zr** as well, the kinetic and thermodynamic products are different, providing thereby another example in which alkene coordination has introduced effects that do not conform to the Evans–Polanyi relation. Such effects can have direct important consequences to the chemistry of C–C and M–C bond formation. Clearly, the reversed regioselectivity in **1-Zr** has potential to expand the utility of reactions involving C–C bond formation by radical addition to substituted alkenes. In systems such as **1-Rh** on the other hand, the retained kinetic preference

(19) While a more thorough analysis of the nature of the asymmetric metal–olefin bond is still needed, the fact that the calculated isobutene adducts of both the [Cp₂Zr(O^tBu)]⁺ and [ZrCl₃]⁺ fragments are asymmetrical suggests that the driving force for the asymmetric bonding mode has a major electronic component. In these systems, the greater steric effects expected from the bulkier Cp ligands appear to be manifested in longer Zr–CH₂ bonds. For example, the Zr–CH₂ bond distance in the isobutene adduct of [ZrCl₃]⁺ is 2.40 Å, compared to 2.69 Å in the isobutene adduct of [Cp₂Zr(O^tBu)]⁺.

(20) Wiberg, K. B.; Raben, P. R. *J. Comput. Chem.* **1993**, *14*, 1504.

for the unsubstituted end of the alkene has potential to open a viable route to making secondary or even tertiary M–C bonds. Although the present study is not tied to any particular experiment, the results and associated discussions should be relevant to understanding free radical addition to metal-coordinated ligands in general, which is an emerging research theme in organometallic chemistry.^{21,22} The two complexes considered in this work represent the limits of d-electron -rich (d^8 -**Rh**) and d-electron-deficient (d^0 -**Zr**) metals. We are cur-

(21) (a) Torraca, K. E.; McElwee-White, L. *Coord. Chem. Rev.* **2000**, 206–207, 469. (b) Matyjaszewski, K.; Xia, J. *Chem. Rev.* **2001**, 101, 2921.

(22) For representative examples see: (a) Ogoshi, S.; Stryker, J. M. *J. Am. Chem. Soc.* **1998**, 120, 3514. (b) Reid, S. J.; Baird, M. C. *Dalton Trans.* **2003**, 20, 3975. (c) Merlic, C. A.; Miller, M. M.; Hietbrink, B. N.; Houk, K. N. *J. Am. Chem. Soc.* **2001**, 123, 4904. (d) Warren, J. J.; Mayer, J. M. *J. Am. Chem. Soc.* **2008**, 130, 2774. (e) Schmalz, H.-G.; Siegel, S.; Bats, J. W. *Angew. Chem., Int. Ed.* **1995**, 34, 2383. (f) Byers, J. H.; Jason, N. J. *Org. Lett.* **2006**, 8, 3455.

rently using the calculations to investigate radical addition to olefins coordinated to transition-metal fragments having systematically varied d^n -metal configurations, geometries, and ligand properties.

Acknowledgment. This work was supported by a grant from the University Research Board at AUB and by an NCSA grant (No. TG-CHE080006N). Professor Alan Goldman is acknowledged for valuable discussions.

Supporting Information Available: Text and tables giving computational details, density functional, solvent, and basis set effects, and DFT vs CCSD-T data for the reaction of isobutene and its $[Li]^+$, $[ZrCl_3]^+$ and $[Rh(PH_3)_2(CH_3)]$ adducts. This material is available free of charge via the Internet at <http://pubs.acs.org>.

OM8007212